



Lung volume determination by dual-source computed tomography in infants with pulmonary artery sling: a case-control study

Qiuyi Cai^{1#^}, Bing Wen^{2#^}, Jianlin Li^{1^}, Liangbo Hu^{3^}, Jian Liu^{1^}, Hao Yang^{1^}

¹Department of Radiology, The Third People's Hospital of Chengdu, Chengdu, China; ²Department of Radiology, Yiyang Central Hospital, Yiyang, China; ³Department of Radiology, The Yongchuan Hospital of Chongqing Medical University, Chongqing, China

Contributions: (I) Conception and design: Q Cai, B Wen; (II) Administrative support: H Yang; (III) Provision of study materials or patients: L Hu; (IV) Collection and assembly of data: Q Cai, J Li; (V) Data analysis and interpretation: B Wen, J Liu; (VI) Manuscript writing: All authors; (VII) Final approval of manuscript: All authors.

[#]These authors contributed equally to this work.

Correspondence to: Hao Yang. Department of Radiology, The Third People's Hospital of Chengdu, Chengdu 610000, China. Email: yhfj129@163.com.

Background: Pulmonary artery sling (PAS) is associated with tracheal stenosis and left pulmonary artery (LPA) dysplasia in infants, both developmental abnormalities that may lead to pulmonary hypoplasia and lung volume changes. As such, we aimed to monitor the effects of tracheal stenosis and pulmonary vascular malformation on lung volumes in infants with PAS and their correlation with lung volumes in infants with PAS using dual-source computed tomography (DSCT).

Methods: A case-control study was performed. From May 2009 to June 2017, we retrospectively enrolled patients with surgically confirmed PAS and compared them to matched normal controls (A healthy control group comprising age- and gender-matched patients with adequate imaging data was used for the comparisons.). All the patients underwent DSCT examinations. We measured and compared the diameters of the trachea, main bronchus, and main pulmonary artery (MPA) and its branches, and both lung volumes on the axial, and reconstructed CT images.

Results: There were no statistical differences in the diameters of the MPA or right pulmonary artery (RPA) between patients (N=15) and controls (N=28). The diameter of the main bronchus, the bilateral trachea and the left pulmonary artery were all smaller in the PAS group than in the control group, and significant differences were evident in the left lung volume the right lung volume, and the right-to-left lung volume ratio between the 2 groups. Pearson's correlation and linear regression analyses between the diameters of the trachea and MPA, total lung volume, ipsilateral bronchial and pulmonary artery branches, and ipsilateral lung volume ranged from 0.71 to 0.87 and 0.57 to 0.77 for the control and PAS groups, respectively.

Conclusions: Tracheal stenosis and LPA dysplasia in infants with PAS cause alterations in lung tissue morphology and physiological development, resulting in reduced bilateral lung volumes.

Keywords: Lung volume; pulmonary artery sling (PAS); dual-source computed tomography (DSCT)

Submitted Feb 21, 2022. Accepted for publication Apr 11, 2022.

doi: 10.21037/tp-22-87

View this article at: <https://dx.doi.org/10.21037/tp-22-87>

[^] ORCID: Qiuyi Cai, 0000-0002-5958-5467; Bing Wen, 0000-0002-7163-1876; Jianlin Li, 0000-0002-5797-8048; Liangbo Hu, 0000-0002-1729-4274; Jian Liu, 0000-0002-2125-0901; Hao Yang, 0000-0003-3121-1612.

Introduction

Pulmonary artery sling (PAS), also known as an aberrant left pulmonary artery (LPA), is a rare malformation with an incidence of 0.14% in congenital heart diseases (1). Clinically, PAS is an important cause of respiratory symptoms in infants and young children. However, the early clinical manifestations of the disease are non-specific, which makes early diagnosis and timely treatment difficult. In PAS, an LPA abnormality originating in the right pulmonary artery (RPA) passes between the distal trachea and esophagus to reach the left lung, forming a sling with the proximal trachea and main bronchus (2,3). It is often associated with lower tracheal abnormalities, right main bronchus stenosis deformity, and esophageal abnormalities that may cause different degrees of oppression, such as choking, coughing, wheezing, and dyspnea. Ventilation disturbance caused by incomplete airway obstruction is the most prominent manifestation, but it can eventually lead to tracheal softening, severe pulmonary hypertension, and other complications (4). In infants and young children, these PAS-related pulmonary vascular and tracheal malformations may cause defects in lung development and lung volume.

Lung volume refers to normal lung development and its available volume. It is one of the main factors affecting the function of lung tissue. Pulmonary function testing (PFT) is the gold standard of lung volume measurement (5-7). However, this type of test has some drawbacks. First, it is difficult for infants and young children to participate willingly in this test. Second, the lung volume measured by PFT includes the gas content of the oral cavity, trachea, and main bronchus, all components that should be excluded when measuring the lung volume. Compared to PFT, dual-source computed tomography (DSCT) is an easily applicable and accurate tool for measuring the lung volume. Indeed, the lung volume measured using DSCT is closer to the true value because quantitative software can be used to calculate the volume of the whole lung or just 1 side of the lung. Conversely, the lung volume measured using PFT includes the gas content of the mouth, trachea, and main bronchus; however, the lung volume should exclude these components. Therefore, a great deal of researches have focused on the measurement and application of computed tomography (CT) to lung volume assessment (8,9). Moreover, there is evidence that CT can show the relationship between blood vessels, the trachea and its branches, and the position, range, and degree of tracheal stenosis (10,11). CT can also help evaluate and diagnose

other cardiac malformations (12). At present, there are few studies that applied DSCT to investigate the relationship between lung volume and pulmonary vascular and tracheal dysplasia in infants with PAS, and the measurements of lung volume in infants with PAS using DSCT may have implications for evaluating the severity of impaired lung function in PAS and for evaluating lung function recovery before and after surgery. Thus, we aimed to use DSCT to measure the lung volume, the diameter of pulmonary blood vessels and trachea of PAS patients to explore the relationship between lung dysplasia and lung volume in children with PAS. We present the following article in accordance with the STROBE reporting checklist (available at <https://tp.amegroups.com/article/view/10.21037/tp-22-87/rc>).

Methods

Study population

In this retrospective study, we collected the data of patients with and without PAS who underwent DSCT between May 2009 to June 2017 in West China women's and children's Hospital. The PAS patients that were confirmed by surgery were included in the analysis, and patients were excluded if they had emphysema, pulmonary dysplasia, or severe pulmonary infection. A healthy control group comprising age- and gender-matched patients with adequate imaging data was used for the comparisons. The West China women's and children's Hospital was informed and agreed with this study and the consent was obtained from the patients' guardians. The study was conducted in accordance with the Declaration of Helsinki (as revised in 2013). The study was approved by the Institutional Ethics Committee of the Third People's Hospital of Chengdu [No. (2020)S-117].

CT image acquisition

All examinations were performed on a DSCT scanner (SOMATOM Definition; Siemens Medical Solutions, Forchheim, Germany). Short-term sedation was administered to patients aged <6 years by an intravenous injection of chloral hydrate (concentration: 10%, 0.5 mL/kg). A non-ionic contrast (iopamidol, 370 mg/mL; Bracco, Sine Pharmaceutical Corp. Ltd., Shanghai China) was injected into an antecubital vein at a rate of 1.2–2.5 mL/s, following 20 mL of saline solution. The injected dose was adjusted based on patients' body weight (1.5 mL/kg).

Scanning was performed from the inlet of the thorax to 2 cm below the diaphragm in a craniocaudal direction. Bolus tracking was used in the descending aorta (Ao) in a region of interest with a predefined threshold of 100 Hounsfield units (HU). Image acquisition was activated following a delay of 5 s, when the attenuation threshold reached 100 HU. A prospective electrocardiography-gated protocol was used with the following acquisition parameters: gantry rotation time, 0.28 s; tube voltage, 80 kV; tube current, 100 mAs and pitch, 0.2–0.5 (selected based on heart rate; a higher pitch was used for higher heart rates).

Image analysis

All the acquired data were processed on a workstation (Syngo; Siemens Medical System, Forchheim, Germany). A slice thickness of 1 mm at 0.75 mm increments was chosen for the image reconstruction. For the image post-processing (e.g., multiplanar reformation), 2 experienced radiologists, who were unaware of the measurement results, independently reviewed each CT image on a dedicated workstation (Leonardo, Siemens Medical Systems). Differences in interpretation were resolved by discussion until a consensus was reached. Finally, we used the average value of the measured results from the 2 radiologists.

Parameters assessed

The measured parameters combined with 3D plane are summarized in *Figure 1A–1E*. The pulmonary artery was assessed on a transverse image in a mediastinal window (13). The vessel diameters were obtained by measuring the widest diameter vertical to the long axis of the main pulmonary artery (MPA) (line 1) using a computer caliper (14–17) (see *Figure 1A*). The diameters of the LPA and RPA were taken at the widest portion distal to the bifurcation (18,19); however, the anatomical location of the variation occurred in pulmonary artery bifurcation (2,3). Thus, we defined a method by making a tangent (line 3) at the opening of the LPA with the axis of the LPA (line 2), when measuring the diameter of the LPA in the PAS group. we measured the vertical distance (line 1) in the axis of pulmonary artery compression at the site of the tracheal stenosis. For the control group, the length of the axis line (line 2) was fixed at 1 cm (see *Figure 1B*). We measured the RPA diameter by making a tangent (line 3) along the right side of the ascending and descending aorta, then drawing a line (line 2) along the long axis of the pulmonary artery, and finally

drawing the vertical line (line 1) of the line 2 from the intersection of the tangent line (line 3) and the pulmonary artery, which is the diameter of the right pulmonary artery (see *Figure 1C*). As tracheal stenosis mainly occurs in the lower trachea, the transverse diameter of the main bronchus (20) was measured at the level of the carina (see *Figure 1D*). In the 3D reconstruction, at the widest position of the left bronchial opening into the carina, a vertical line (line 1) was drawn perpendicular to the long axis (line 2) of the trachea (21) (see *Figure 1E*). The diameter of the contralateral bronchus was measured using the same method. The window and level were adjusted as necessary.

Using dedicated software (Lung Density, Philips Medical System), the left and right lung volumes were measured and recorded semiautomatically using a 3D approach. Semiautomatic segmentation was based on fixed density thresholds (lower threshold: –1,024 HU; upper threshold: –200 HU) with a 1-mm thickness starting from the apex and spreading over the lung boundary. Finally, the system automatically calculated the lung volumes on each side and on 3 occasions, and the average value was taken (see *Figure 2*).

Statistical analysis

The statistical analysis was performed using the SPSS statistics, Version 17.0 (SPSS Institute Inc., Chicago, IL, USA) and MedCalc Version 9.3.0.0 (MedCalc software, Mariakerke, Belgium). The dichotomous data are expressed as numbers and percentages, while the continuous variables are expressed as means \pm standard deviations. Volumes and diameters with normal distributions and homogeneity of variance were analyzed for significant differences between the case and control patients using independent sample *t*-tests. Spearman correlation and linear regression analyses were used to evaluate the relationships between the diameter and volume in these 2 groups. The Pearson's correlation coefficient was calculated with 95% confidence intervals. A 2-tailed *P* value <0.05 was considered statistically significant.

Results

Patients' characteristics

We included 49 subjects in this study who underwent DSCT but excluded 6 patients because of emphysema, pulmonary dysplasia, or severe pulmonary infection. Thus, 15 patients with PAS (7 boys and 8 girls; mean age, 8.87 ± 5.08 months)

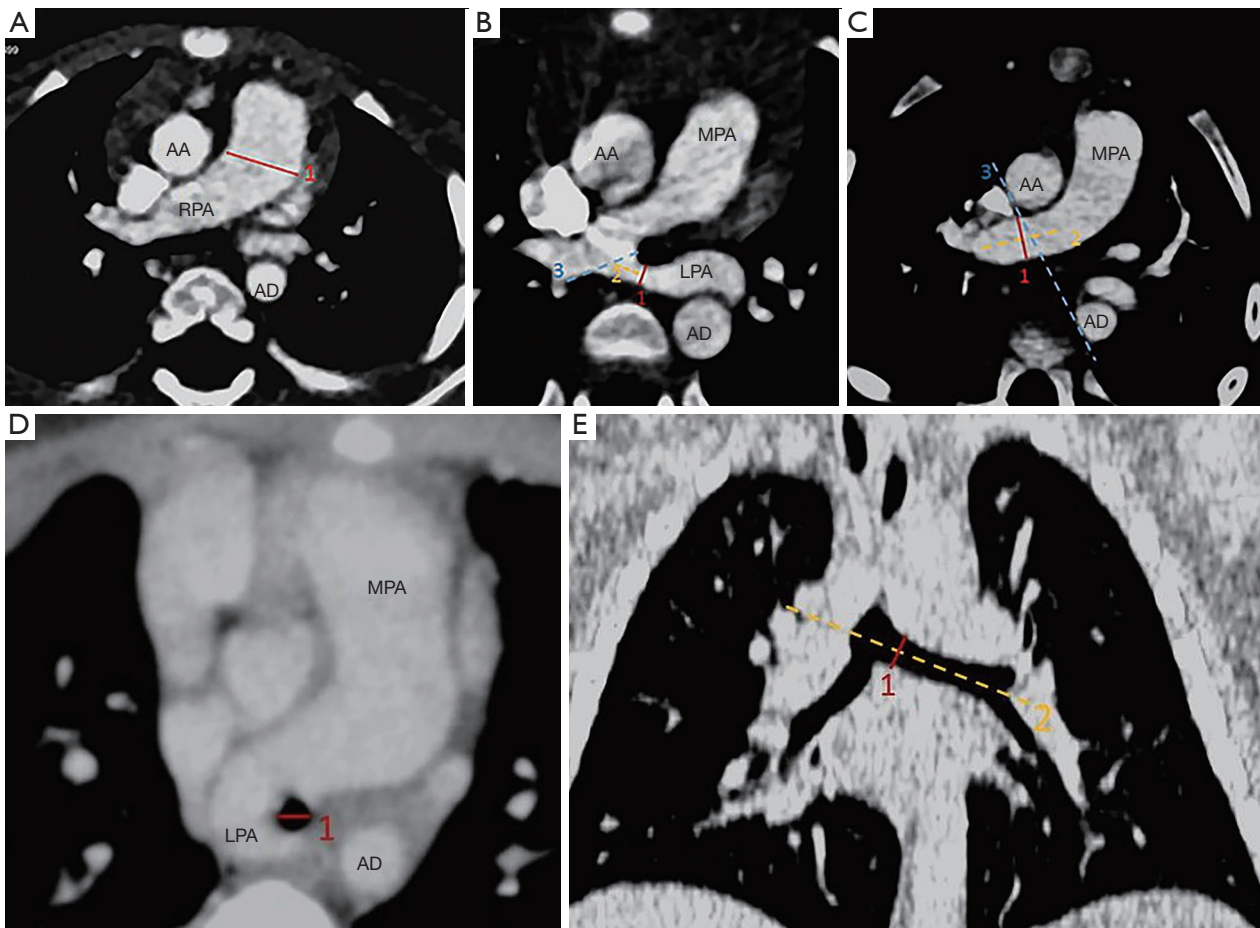


Figure 1 A set of images about the measured trajectories of the aorta, pulmonary artery and trachea. A shows the pulmonary artery diameter (line 1); B shows the diameter of the left pulmonary artery (line 1), a line tangent to the opening of the left pulmonary artery (line 3), and a line parallel to the long axis of the left pulmonary artery (line 2); C shows the diameter of the right pulmonary artery (line 1) tangent to the right border of the ascending and descending aorta (line 3) and a line parallel to the long axis of the right pulmonary artery (line 2); D shows the trachea diameter (line 1); E shows the diameter of left bronchus (line 1), the long axis of the left trachea (line 2). AA, aorta ascendens; AD, aorta descendens; MPA indicates main pulmonary artery; LPA, left pulmonary artery; RPA, right pulmonary artery.

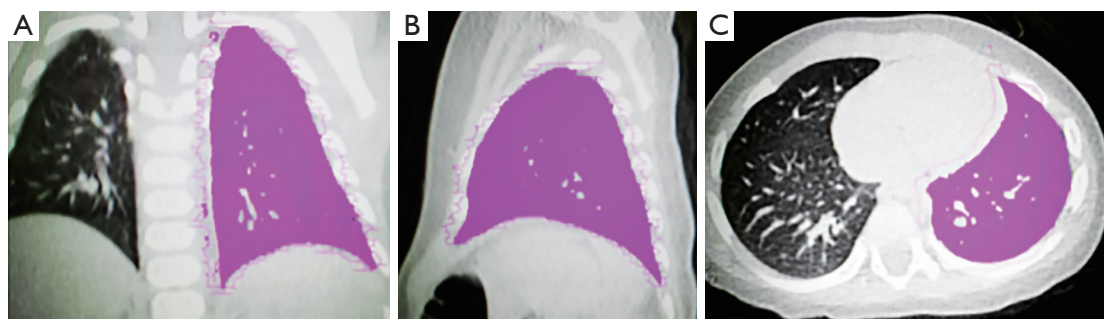


Figure 2 Measurement of left lung volumes in different planes (the pink area represents the lung volume measurement range). Schematic diagram of coronal position (A), sagittal position (B), and transverse position (C).

Table 1 Baseline characteristics of the PAS and control groups

Clinical characteristics	PAS (N=15)	Controls (N=28)	P value
Age, months	8.87±5.08	9.14±5.09	0.87
Gender (male:female)	7:8	1:1	–
Weight (kg)	7.44±1.40	7.63±1.50	0.71
Height (cm)	66.43±5.06	67.29±5.28	0.61
BMI	16.80±1.93	16.83±2.52	0.97
PAS	15	0	–
Ventricular septal defect	3	0	–
Atrial septal defect	7	0	–
SLVC	1	0	–
BAV	1	0	–
PDA	1	0	–
Pulmonary absent	0	0	–
Emphysema pulmonum	0	0	–

PAS, pulmonary artery sling; BMI, body mass index; SLVC, persistent left superior vena cava; BAV, bicuspid aortic valve; PDA, patent ductus arteriosus.

and 28 healthy subjects (14 boys and 14 girls; mean age, 9.14±5.09 months) were enrolled in the study. High-quality images (in which the anatomic details were clearly visible) were obtained for all the patients for the imaging analysis. Age, weight, height, and body mass index did not differ significantly between the PAS and control groups (all $P>0.05$). Among the 15 patients with PAS, 7 had atrial septal defects, 3 had ventricular septal defects, 1 had a double superior vena cava, 1 had patent ductus arteriosus, and 1 had bicuspid aortic valve (see *Table 1*).

Measurements of the 2 groups

The measurement data are summarized in *Table 2*. The above data conform to the normal distribution, and the independent sample *t*-test is used. Among the parameters measured, the left and right lung volumes and the diameters of the trachea, left bronchus, right bronchus, and LPA were significantly smaller in the PAS group than the control group. Additionally, the right-to-left lung volume ratios differed significantly between the 2 groups. However, the diameters of MPA and RPA did not differ significantly

Table 2 Comparison of measurements between the PAS and control groups

Measurement area	PAS	Controls	P value
Tracheal	0.44±0.11	0.91±0.13	0.000
Left bronchus	0.29±0.08	0.40±0.10	0.000
Right bronchus	0.35±0.07	0.46±0.08	0.000
Pulmonary trunk	1.39±0.14	1.35±0.12	0.327
Left pulmonary artery	0.35±0.09	0.89±0.10	0.000
Right pulmonary artery	0.93±0.12	0.96±0.12	0.342
Left lung volume	105.45±29.66	144.41±31.97	0.000
Right lung volume	139.43±39.05	174.49±39.72	0.008
RV/LV	1.33±0.14	1.21±0.07	0.004

PAS, pulmonary artery sling; RV, right lung volume; LV, left lung volume.

between the PAS and control groups.

Correlation analysis between the dimension and volume

The results of the Pearson correlation and linear regression analyses between the tracheal or MPA diameter and the total lung, left lung, and right lung volumes with the parameters are summarized in *Table 3* and *Figure 3*. There was a significant positive correlation between main bronchial diameter and total lung volume, right bronchial diameter and right lung volume, and left bronchial diameter and left lung volume; similarly, there was a high correlation between main pulmonary artery diameter and total lung volume, right pulmonary artery diameter and right lung volume, and left pulmonary artery diameter and left lung volume ($r=0.71$ – 0.87 ; all $P<0.001$) in the control group, but each correlation was lower ($r=0.57$ – 0.77 ; all $P<0.05$) in the PAS group.

Associated malformations

Of the 15 infants with PAS, 13 had associated malformations that were surgically confirmed. The DSCT findings are summarized in *Table 4*. The diagnostic accuracy of DSCT for PAS was 100% (15/15), but the DSCT failed to diagnose 1 bicuspid pulmonary valve (0/1) and 2 atrial septal defects (5/7). Thus, the diagnostic accuracy of DSCT for detecting PAS patients' associated with cardiac malformations was 76.92% (10/13).

Table 3 Correlation of data by PAS groups according to lung volume

Region	PAS group					
	Total LV		LLV		RLV	
	r	P value	r	P value	r	P value
Tracheal	0.59	0.0199				
Left bronchus			0.57	0.0275		
Right bronchus					0.69	0.0047
MPA	0.62	0.0142				
LPA			0.59	0.0203		
RPA					0.77	0.0007

PAS, pulmonary artery sling; MPA indicates main pulmonary artery; LPA, left pulmonary artery; RPA, right pulmonary artery; LV, lung volume; LLV, left lung volume; RLV, right lung volume; r, rank correlation coefficient.

Discussion

Main findings

The results of this study indicate that between patients with PAS and healthy controls, the diameters of MPA and RPA were similar, but there were significant differences in the diameters of the trachea and LPA and in the volumes of the left and right lungs. Clinically, the tracheas were stenosed, and the LPAs were smaller in patients with PAS. More importantly, the bilateral lung volumes were concomitantly reduced.

Morphological characteristics

PAS was first reported by Glaevecke and Doehle (22). Embryologically, the disorder results from LPA dysplasia,

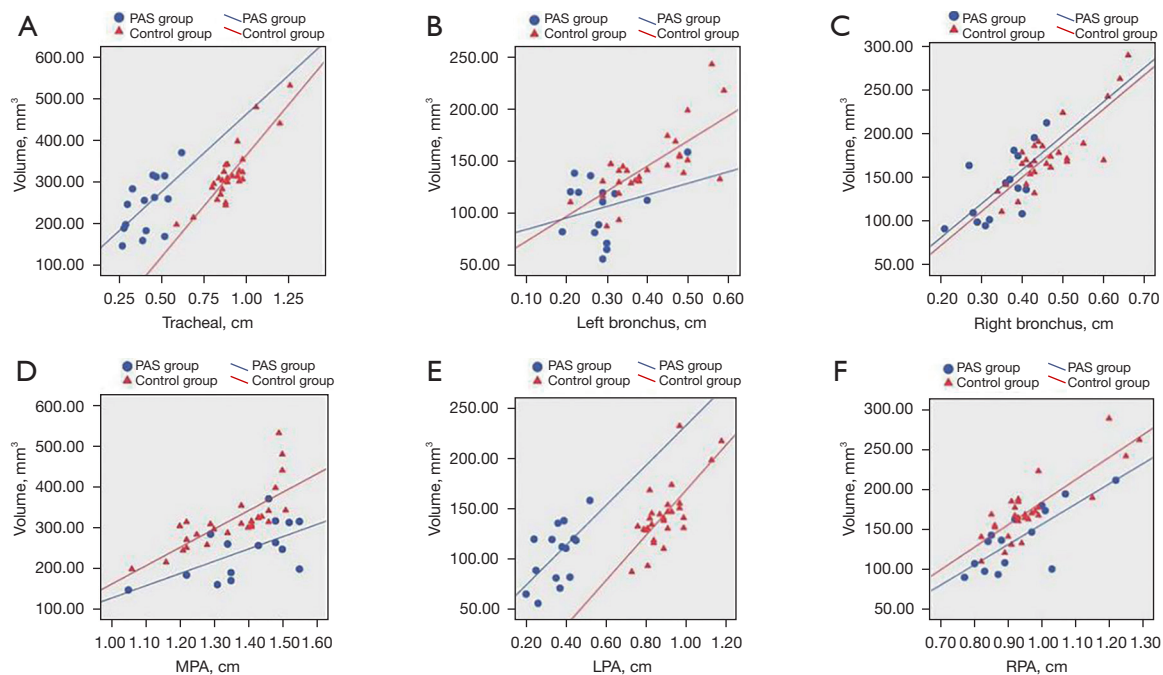


Figure 3 Statistical results of the PAS and control groups. Scattergrams for the PAS and control groups showing the linear regression results between the tracheal and total lung volume (A), left bronchus and left lung volume (B), right bronchus and right lung volume (C), MPA and total lung volume (D), the LPA and left lung volume (E), and the RPA and right lung volume (F). The Pearson's correlation coefficients in the PAS group were $r=0.59$ ($P=0.0199$), $r=0.57$ ($P=0.0275$), and $r=0.69$ ($P=0.0047$), respectively; in the control group, they were $r=0.87$ ($P<0.001$), $r=0.72$ ($P<0.001$), and $r=0.83$ ($P<0.001$), respectively. In the PAS group, the results were $r=0.62$ ($P<0.05$), $r=0.59$ ($P<0.05$), and $r=0.77$ ($P<0.001$), respectively. In the control group, the results were $r=0.76$ ($P<0.001$), $r=0.71$ ($P<0.001$), and $r=0.84$ ($P<0.001$), respectively. PAS, Pulmonary artery sling; MPA indicates main pulmonary artery; LPA, left pulmonary artery; RPA, right pulmonary artery.

Table 4 The diagnostic accuracies of DSCT by anomaly

Group	PAS	PDA	ASD	VSD	SLVC	BAV
DSCT findings	15	1	5	3	1	0
Surgical results	15	1	7	3	1	1

DSCT, dual source computed tomography; PAS, pulmonary artery sling; PDA, patent ductus arteriosus; ASD, atrial septal defect; VSD, ventricular septal defect; SLVC, persistent left superior vena cava; BAV, bicuspid aortic valve.

which affects the normal development of the tracheobronchial tree and the left bow (23). Pathologically, the LPA is unable to connect with the 6th bow of the left side of the aorta in the embryonic period, resulting in an anomalous connection with the right vascular bud via post-branchial channels between the trachea and esophagus. The compression of the trachea and esophagus or extensive tracheal or bronchial stenosis then causes subsequent clinical symptoms. Among the congenital heart diseases that can cause tracheal stenosis, the bronchial stenosis of PAS is the most serious (24). The PAS can be combined with a patent ductus arteriosus. When the patent ductus arteriosus and the abnormal left pulmonary artery form a complete vascular ring, it can cause compression on the trachea and bronchi. In such cases, PAS can clinically manifest as significant esophageal and tracheal symptoms (2,3,25). Of the 15 patients in this study, 1 (7%) had a complete vascular ring.

Quantitative measurements

We found that the transverse diameter of the main bronchus and its branches decreased by different degrees in the PAS group. Tracheal stenosis and bronchomalacia often occur in association with pulmonary agenesis (26). Additionally, the correlation of the trachea and its branch diameters with the lung volume also decreased by varying degrees (0.57–0.69 vs. 0.72–0.87, respectively). Virtual bronchoscopy grading of tracheobronchial stenosis has been found to correlate well with PFT results, indicating that tracheal stenosis will increase airway resistance (27). This can cause pulmonary ventilation disturbances (28) and different degrees of hypoxia in the lungs, ultimately affecting lung development directly (29). For example, studies have shown that subjecting pregnant rats to hypoxia causes reductions in lung dry weight, lung content, and protein content in fetal rats, thereby decreasing pulmonary surfactant expression. Thus, hypoxia reduces the total number of cells and inhibits the development of vascular and alveolar epithelia and can

arrest lung development (30,31), potentially reducing lung volume.

It was expected that the LPA diameter of patients with PAS would be smaller than that of the control group. Embryologically, pulmonary artery hypoplasia results from the failed development of the 6th aortic arch. The lungs originate as a pair of lung buds from the foregut endoderm and interact with the developing pulmonary vessels (32–34). The capillaries of the early lung buds originate from the primitive systemic circulation, but as the lungs grow, these primitive systemic vessels regress. In later lung development, good perfusion of the capillary bed is essential for alveoli to form (35,36). Finally, the vascular changes in PAS may cause the lung bud to be inadequately perfused and to become ischemic, causing lung agenesis because of the complete arrest of the pulmonary arterial supply. The view that pulmonary hypoplasia is attributable to pulmonary artery hypoplasia is supported by evidence that a reduction in pulmonary blood flow prevents lung development and causes lung hypoplasia (37,38).

In the control group, we found that the diameter of MPA and the bilateral lung volumes, the diameter of LPA and the left lung volumes, and the diameter of RPA and the right lung volume have a significant association ($r=0.71-0.84$; all $P<0.0001$). In addition, Other studies have also found that the diameter of LPA has a significant association with gestational age (39,40), and the total lung volume has a significant association with gestational age as well (41,42). Thus, the normal fetal MPA and its branches have a good correlation with both lung volumes. This is consistent with our results, which showed varying degrees of decline in the PAS group ($r=0.59-0.77$; all $P<0.05$). Additionally, some heart abnormalities associated with PAS are caused by lung development (43). We conclude that decreases in both lung volumes must result from a complex interaction between the tracheal stenosis, small LPA, and concurrent cardiac malformations.

The CT value reflects the density change of tissue and is determined by the gas, blood, and lung tissue in the lungs (44). The function of fetal lung tissue depends on proper lung development and an appropriate lung volume (42). In this study, we used the domain value of the segmentation technology to determine the lung volume using software. There are many reports about the choice of domain value. For example, some research (45) has shown that volume software was better able to isolate lung tissue when the multi-slice CT threshold was set from $-1,024$ to -200 HU; however, some manual correction was needed

to remove the trachea and blood vessels to improve the detection accuracy. Nevertheless, it appears that there is a high correlation between lung volume and function with this technique. The decrease in lung volume in patients with PAS implies that pulmonary function is also reduced, which is of significance when evaluating pulmonary function by measuring the lung volume pre- and post-operatively.

In this cohort, the diagnostic accuracy of DSCT was 73.68% (10/13). DSCT failed to diagnose several small anomalies, including a bicuspid pulmonary valve (0/1), an atrial septal defect (3/4), and a foramen ovale defect (2/3). This may be because DSCT imaging is a digital-based technology requiring a workstation to hide digital information from the grey-level images. Unfortunately, some intracardiac abnormalities are too small to sharply and clearly demonstrate using this method, and we cannot make an accurate judgement of whether a deformity exists. Thus, an important diagnosis may be missed.

Limitations

This study had several limitations. First, due to the very low incidence of this disease, we were only able to include a small number of patients in the study, which limits our ability to extrapolate the results. Second, we did not compare our measurements with the results of PFT because in this retrospective study, we had no access to these clinical measurements. Third, there was a lack of long-term follow-up data on heart and lung function after surgery, as some of the patients in this study died or could not be contacted.

Conclusions

Patients with PAS not only have a small LPA and tracheal stenosis but also frequently have decreased left and right pulmonary volumes. This shows that PAS is a complicated deformity that causes lung underdevelopment. In addition to causing tracheal stenosis, PAS decrease lung volume of infants, affecting their lung function and normal breathing.

Acknowledgments

The authors acknowledge support from the Department of Radiology of West China Women's and Children's Hospital. *Funding:* This work was supported by The Natural Science Fund of Yongchuan District, Chongqing. (grant No. Ycstc, 2015nc5010 to Liangbo Hu).

Footnote

Reporting Checklist: The authors have completed the STROBE reporting checklist. Available at <https://tp.amegroups.com/article/view/10.21037/tp-22-87/rc>

Data Sharing Statement: Available at <https://tp.amegroups.com/article/view/10.21037/tp-22-87/dss>

Conflicts of Interest: All authors have completed the ICMJE uniform disclosure form (available at <https://tp.amegroups.com/article/view/10.21037/tp-22-87/coif>). Liangbo Hu reports funding from the Natural Science Fund of Yongchuan District, Chongqing. (grant No. Ycstc, 2015nc5010). The other authors have no conflicts of interest to declare.

Ethical Statement: The authors are accountable for all aspects of the work in ensuring that questions related to the accuracy or integrity of any part of the work are appropriately investigated and resolved. The study was conducted in accordance with the Declaration of Helsinki (as revised in 2013). The study was approved by the Institutional Ethics Committee of the Third People's Hospital of Chengdu [No. (2020)S-117] and informed consent was taken from the patients' guardians.

Open Access Statement: This is an Open Access article distributed in accordance with the Creative Commons Attribution-NonCommercial-NoDerivs 4.0 International License (CC BY-NC-ND 4.0), which permits the non-commercial replication and distribution of the article with the strict proviso that no changes or edits are made and the original work is properly cited (including links to both the formal publication through the relevant DOI and the license). See: <https://creativecommons.org/licenses/by-nc-nd/4.0/>.

References

1. Xie J, Juan YH, Wang Q, et al. Evaluation of left pulmonary artery sling, associated cardiovascular anomalies, and surgical outcomes using cardiovascular computed tomography angiography. *Sci Rep* 2017;7:40042.
2. Lee M, Landsem L. Pulmonary Artery Sling. In: *StatPearls*. Treasure Island (FL): StatPearls Publishing; September 3, 2020.
3. Sezer S, Acar DK, Ekiz A, et al. Prenatal diagnosis of left pulmonary artery sling and review of literature.

- Echocardiography 2019;36:1001-4.
4. Yong MS, d'Udekem Y, Brizard CP, et al. Surgical management of pulmonary artery sling in children. *J Thorac Cardiovasc Surg* 2013;145:1033-9.
 5. Monroy-Cárdenas MA, Hernández-Sarmiento R, Barón-Puentes OU. Pulmonary artery sling in preschool patient with airway compromise. *Bol Med Hosp Infant Mex* 2019;76:241-5.
 6. Kloth C, Maximilian Thaiss W, Preibsch H, et al. Quantitative chest CT analysis in patients with systemic sclerosis before and after autologous stem cell transplantation: comparison of results with those of pulmonary function tests and clinical tests. *Rheumatology (Oxford)* 2016;55:1763-70.
 7. Kim SS, Seo JB, Lee HY, et al. Chronic obstructive pulmonary disease: lobe-based visual assessment of volumetric CT by Using standard images--comparison with quantitative CT and pulmonary function test in the COPDGene study. *Radiology* 2013;266:626-35.
 8. Shi K, Gao HL, Yang ZG, et al. Dual-source computed tomography for quantitative assessment of tracheobronchial anomaly from type IIA pulmonary artery sling in pediatric patients. *Eur J Radiol* 2018;102:30-5.
 9. Leitman EM, McDermott S. Pulmonary arteries: imaging of pulmonary embolism and beyond. *Cardiovasc Diagn Ther* 2019;9:S37-58.
 10. Wang SY, Gao W, Zhong YM, et al. Multislice Computed Tomography Assessment of Tracheobronchial Patterns in Partial Anomalous Left Pulmonary Artery. *J Comput Assist Tomogr* 2017;41:983-9.
 11. Zhong YM, Jaffe RB, Zhu M, et al. CT assessment of tracheobronchial anomaly in left pulmonary artery sling. *Pediatr Radiol* 2010;40:1755-62.
 12. Ihlenburg S, Rompel O, Rueffer A, et al. Dual source computed tomography in patients with congenital heart disease. *Thorac Cardiovasc Surg* 2014;62:203-10.
 13. Greenberg SB, Lang SM, Gauss CH, et al. Normal pulmonary artery and branch pulmonary artery sizes in children. *Int J Cardiovasc Imaging* 2018;34:967-74.
 14. Lee SH, Kim YJ, Lee HJ, et al. Comparison of CT-Determined Pulmonary Artery Diameter, Aortic Diameter, and Their Ratio in Healthy and Diverse Clinical Conditions. *PLoS One* 2015;10:e0126646.
 15. McCall RK, Ravenel JG, Nietert PJ, et al. Relationship of main pulmonary artery diameter to pulmonary arterial pressure in scleroderma patients with and without interstitial fibrosis. *J Comput Assist Tomogr* 2014;38:163-8.
 16. Heinrich M, Uder M, Tscholl D, et al. CT scan findings in chronic thromboembolic pulmonary hypertension: predictors of hemodynamic improvement after pulmonary thromboendarterectomy. *Chest* 2005;127:1606-13.
 17. Iyer AS, Wells JM, Vishin S, et al. CT scan-measured pulmonary artery to aorta ratio and echocardiography for detecting pulmonary hypertension in severe COPD. *Chest* 2014;145:824-32.
 18. Lange TJ, Dornia C, Stiefel J, et al. Increased pulmonary artery diameter on chest computed tomography can predict borderline pulmonary hypertension. *Pulm Circ* 2013;3:363-8.
 19. Chen X, Liu K, Wang Z, et al. Computed tomography measurement of pulmonary artery for diagnosis of COPD and its comorbidity pulmonary hypertension. *Int J Chron Obstruct Pulmon Dis* 2015;10:2525-33.
 20. Thierry B, Luscan R. Use of Computed Tomography Scan in Pediatric Bronchial Measurements. *J Cardiothorac Vasc Anesth* 2021;35:1553-4.
 21. Mi W, Zhang C, Wang H, et al. Measurement and analysis of the tracheobronchial tree in Chinese population using computed tomography. *PLoS One* 2015;10:e0123177.
 22. Glaevecke H, Doehle W. Über eine seltene angeborene Anomalie der Pulmonalarterie. *Munch Med Wochenschr* 1897;44:950-3.
 23. Fukushima N, Shimojima N, Ishitate M, et al. Clinical and structural aspects of tracheal stenosis and a novel embryological hypothesis of left pulmonary artery sling. *Pediatr Pulmonol* 2020;55:747-53.
 24. Loukanov T, Sebening C, Springer W, et al. Simultaneous management of congenital tracheal stenosis and cardiac anomalies in infants. *J Thorac Cardiovasc Surg* 2005;130:1537-41.
 25. Berdon WE, Muensterer OJ, Zong YM, et al. The triad of bridging bronchus malformation associated with left pulmonary artery sling and narrowing of the airway: the legacy of Wells and Landing. *Pediatr Radiol* 2012;42:215-9.
 26. Stephens EH, Eltayeb O, Mongé MC, et al. Pediatric Tracheal Surgery: A 25-Year Review of Slide Tracheoplasty and Tracheal Resection. *Ann Thorac Surg* 2020;109:148-53.
 27. Qi S, Li Z, Yue Y, et al. Computational fluid dynamics simulation of airflow in the trachea and main bronchi for the subjects with left pulmonary artery sling. *Biomed Eng Online* 2014;13:85.
 28. Shitrit D, Valdislav P, Grubstein A, et al. Accuracy of virtual bronchoscopy for grading tracheobronchial stenosis: correlation with pulmonary function test and fiberoptic bronchoscopy. *Chest* 2005;128:3545-50.

29. Been JV, Zoer B, Kloosterboer N, et al. Pulmonary vascular endothelial growth factor expression and disaturated phospholipid content in a chicken model of hypoxia-induced fetal growth restriction. *Neonatology* 2010;97:183-9.
30. Tsao PN, Wei SC. Prenatal hypoxia downregulates the expression of pulmonary vascular endothelial growth factor and its receptors in fetal mice. *Neonatology* 2013;103:300-7.
31. Coffin JD, Poole TJ. Embryonic vascular development: immunohistochemical identification of the origin and subsequent morphogenesis of the major vessel primordia in quail embryos. *Development* 1988;102:735-48.
32. Kina YP, Khadim A, Seeger W, et al. The Lung Vasculature: A Driver or Passenger in Lung Branching Morphogenesis? *Front Cell Dev Biol* 2020;8:623868.
33. Stenmark KR, Gebb SA. Lung vascular development: breathing new life into an old problem. *Am J Respir Cell Mol Biol* 2003;28:133-7.
34. Hislop AA. Airway and blood vessel interaction during lung development. *J Anat* 2002;201:325-34.
35. Weibel ER. Lung morphometry: the link between structure and function. *Cell Tissue Res* 2017;367:413-26.
36. Vitiello R, Pisanti C, Pisanti A, et al. Association of pulmonary artery agenesis and hypoplasia of the lung. *Pediatr Pulmonol* 2006;41:897-9.
37. Sunam G, Ceran S. Pulmonary artery agenesis and lung hypoplasia. *Eur J Gen Med* 2009;6:265-7.
38. Achiron R, Golan-Porat N, Gabbay U, et al. In utero ultrasonographic measurements of fetal aortic and pulmonary artery diameters during the first half of gestation. *Ultrasound Obstet Gynecol* 1998;11:180-4.
39. Katayama S, Tada K, Nakanishi Y, et al. Evaluation of normal fetal branch pulmonary artery diameters measured by ultrasonography: a comparison with congenital diaphragmatic hernia. *Fetal Diagn Ther* 2008;23:303-7.
40. Tang Y, Jin XD, Xu L, et al. The Value of Ultrasonography in Assessing Fetal Lung Maturity. *J Comput Assist Tomogr* 2020;44:328-33.
41. Liu JD, Bing G, Xue C. Four-dimensional ultrasonography measured lung volume in predicting pulmonary hypoplasia of fetus. 2012 International Conference on Biomedical Engineering and Biotechnology, 2012:1490-2.
42. Ruchonnet-Metrailler I, Bessieres B, Bonnet D, et al. Pulmonary hypoplasia associated with congenital heart diseases: a fetal study. *PLoS One* 2014;9:e93557.
43. Johnson JL, Kramer SS, Mahboubi S. Air trapping in children: evaluation with dynamic lung densitometry with spiral CT. *Radiology* 1998;206:95-101.
44. Jian JQ, Deng DY, Wan L, et al. Characteristic Changes and 3D Virtual Measurement of Lung CT Image Parameters in the Drowning Rabbit Model. *Fa Yi Xue Za Zhi* 2019;35:1-4.
45. Kauczor HU, Heussel CP, Fischer B, et al. Assessment of lung volumes using helical CT at inspiration and expiration: comparison with pulmonary function tests. *AJR Am J Roentgenol* 1998;171:1091-5.

Cite this article as: Cai Q, Wen B, Li J, Hu L, Liu J, Yang H. Lung volume determination by dual-source computed tomography in infants with pulmonary artery sling: a case-control study. *Transl Pediatr* 2022;11(4):565-574. doi: 10.21037/tp-22-87